Dynamical quantum phase transitions in discrete time crystals

Arkadiusz Kosior[1] and Krzysztof Sacha[1,2]
[1]*Instytut Fizyki imienia Mariana Smoluchowskiego, Uniwersytet Jagielloński, ulica Profesora Stanisława Łojasiewicza 11, PL-30-348 Kraków, Poland*
[2]*Mark Kac Complex Systems Research Center, Uniwersytet Jagielloński, ulica Profesora Stanisława Łojasiewicza 11, PL-30-348 Kraków, Poland*

(Received 20 December 2017; revised manuscript received 1 March 2018; published 29 May 2018)

Discrete time crystals are related to nonequilibrium dynamics of periodically driven quantum many-body systems where the discrete time-translation symmetry of the Hamiltonian is spontaneously broken into another discrete symmetry. Recently, the concept of phase transitions has been extended to nonequilibrium dynamics of time-independent systems induced by a quantum quench, i.e., a sudden change of some parameter of the Hamiltonian. There, the return probability of a system to the ground state reveals singularities in time which are dubbed dynamical quantum phase transitions. We show that the quantum quench in a discrete time crystal leads to dynamical quantum phase transitions where the return probability of a periodically driven system to a Floquet eigenstate before the quench reveals singularities in time. It indicates that dynamical quantum phase transitions are not restricted to time-independent systems and can be also observed in systems that are periodically driven. We discuss how the phenomenon can be observed in ultracold atomic gases.

DOI: 10.1103/PhysRevA.97.053621

I. INTRODUCTION

Phase transitions in equilibrium statistical physics are related to abrupt changes of macroscopic properties of many-body systems [1,2]. Macroscopic quantities that characterize systems in the thermodynamic limit reveal nonanalytical behavior as a function of a control parameter. The equilibrium phase transitions are much better understood than nonequilibrium dynamics of quantum many-body systems [3–13]. Recently, it has been shown that real-time evolution of time-independent many-body systems, after a quantum quench, can reveal nonanalytical behavior at a critical time [14–26]. That is, starting with a system in the ground state, a sudden change of some parameter of the Hamiltonian results in nonanalytical evolution of the return probability to the initial ground state. This phenomenon has been termed dynamical quantum phase transition and it has been already demonstrated in experiments [27,28]; for review see Ref. [29].

In 2012, Frank Wilczek suggested that periodic structures in time could be formed spontaneously by a quantum many-body system [30]. The original idea of such a time crystal could not be realized because it assumed a system in the ground state [31–36]. However, soon it turned out that periodically driven quantum many-body systems were able to self-reorganize their motion and spontaneously start evolving with a period which was different than a period of an external driving [37–48]. These quantum phenomena are dubbed discrete time crystals because discrete time-translation symmetry is broken into another discrete symmetry. Discrete time crystals have been recently observed experimentally [49–51]. It should be stressed that in the classical regime, breaking of discrete time-translation symmetry in an atomic system has been also demonstrated in a laboratory [52,53]. Wilczek's idea initiated a new research area where nontrivial crystalline structures are investigated in the time domain [54–64]; for review see Ref. [65].

Discrete time crystal formation takes place if interactions between particles are sufficiently strong. If they are not, exact many-body Floquet eigenstates evolve with a period of an external driving and are not vulnerable to infinitesimally weak perturbations. However, when the strength of particle interactions is greater than a critical value, Floquet eigenstates possess Schrödinger cat like structures and any perturbation, or even measurement of a position of a single particle, has a dramatic effect on system dynamics leading to a change of the period of motion [37,65]. Here we will show that starting with a Floquet eigenstate in the regime of time crystal formation, an abrupt change of the particle interaction strength to the weak interaction regime induces dynamical quantum phase transitions. That is, the return probability to the initial Floquet eigenstate reveals singularities in time. In the second part of the article, we consider singularities in the dynamics of states with spontaneously broken time-translation symmetry, and identify experimentally measurable observables.

II. RESULTS

We will focus on the discrete time crystal described in Ref. [37], i.e., on ultracold bosonic atoms bouncing on a harmonically oscillating (with frequency ω) mirror in the presence of the gravitational force [66–69]. Let us begin with a single particle problem. In the frame moving with the mirror and in the gravitational units, the Hamiltonian for a single-particle system reads $H_0 = \frac{p^2}{2} + x + \Lambda x \cos(\omega t)$ where $x \geqslant 0$, i.e., the mirror is located at $x = 0$ in the moving frame, and $\frac{\Lambda}{\omega^2}$ is the amplitude of the mirror oscillations in the laboratory frame [69]. Classical description of a single particle reveals resonant periodic orbits with periods equal to integer multiples of the driving period $\frac{2\pi}{\omega}$. We will concentrate on the 2:1 resonance where the classical resonant orbit possesses the period $2\frac{2\pi}{\omega}$.

In the quantum description, there exist two Floquet eigenstates which are represented by two orthogonal superpositions, $u_{1,2}(x,t) \propto \phi_1 \pm \phi_2$, of two localized wave packets, $\phi_{1,2}(x,t)$, that move along the 2:1 resonant orbit like a classical particle. Each of these two wave packets evolves with the period $2\frac{2\pi}{\omega}$, but because after every period $\frac{2\pi}{\omega}$ they exchange their roles, the Floquet eigenstates $u_{1,2}$ are periodic with the period of the external driving. The two Floquet states are eigenstates of the single particle Floquet Hamiltonian, $(H_0 - i\partial_t)u_{1,2} = \varepsilon_{1,2}u_{1,2}$, corresponding to quasienergies $\varepsilon_2 = \varepsilon_1 + J$ (modulo $\frac{\omega}{2}$), where J is an amplitude related to tunneling of a particle from one of the wave packet to the other one.

To find many-body Floquet eigenstates for ultracold atoms bouncing on the oscillating mirror, we assume that interaction energy per particle is much smaller than the energy gap for excitation of the localized wave packets. In the following, we use the parameters as in Ref. [37], i.e., $\Lambda = 0.06$ and $\omega = 1.1$, then the energy gap is about $10^3 J$ while the interaction energy we consider is of the order of $10J$. Therefore, we may restrict to the consideration of behavior of the N-body system in the Hilbert subspace spanned by Fock states $|N-n,n\rangle$, where $N-n$ and n are occupations of the localized wave packets ϕ_1 and ϕ_2, respectively [37,55]. This approximation resembles the two-mode approximation known in the description of a many-body system in a double-well potential [70]. In the time-dependent two-mode basis, $\{\phi_1(x,t),\phi_2(x,t)\}$, our N-body Floquet Hamiltonian reduces to

$$\hat{H} = -\frac{J}{2}(\hat{a}_1^\dagger\hat{a}_2 + \hat{a}_2^\dagger\hat{a}_1) + \frac{U}{2}(\hat{a}_1^\dagger\hat{a}_1^\dagger\hat{a}_1\hat{a}_1 + \hat{a}_2^\dagger\hat{a}_2^\dagger\hat{a}_2\hat{a}_2) + 2U_{12}\hat{a}_1^\dagger\hat{a}_1\hat{a}_2^\dagger\hat{a}_2, \quad (1)$$

where the standard bosonic operators $\hat{a}_{1,2}$ annihilate particles in the modes $\phi_{1,2}$, $U = g_0\int_0^{4\pi/\omega} dt \int_0^\infty dx|\phi_{1,2}|^4$ and $U_{12} = g_0\int_0^{4\pi/\omega} dt \int_0^\infty dx|\phi_1|^2|\phi_2|^2$ with g_0 determined by s-wave scattering length of atoms [37]. For very weak interactions, i.e. for $\gamma = N(U-2U_{12})/J \approx 0$, the ground state of the Hamiltonian Eq. (1) corresponds to a Bose-Einstein condensate where all bosons occupy the single particle Floquet state $u_1(x,t)$. However, if particle interactions are attractive ($g_0 < 0$) and sufficiently strong, $\gamma \ll -1$, it is energetically favorable to group all atoms in one of the localized wave packets. Then, for large N, low-lying eigenstates of the Hamiltonian Eq. (1) are dominated by pairs of nearly degenerate Schrödinger catlike states [71,72]. For example, the lowest two eigenstates of Eq. (1) are $|\psi_\pm(t)\rangle \approx (|N,0\rangle \pm |0,N\rangle)/\sqrt{2}$. Such many-body Floquet eigenstates evolve with the period of the external driving $\frac{2\pi}{\omega}$. However, even if the many-body system is prepared initially in one of such Schrödinger catlike states, e.g., in the Floquet eigenstate $|\psi_+\rangle$, measurement of a position of a single particle leads to a collapse of the eigenstate to $|N,0\rangle$ or $|0,N\rangle$ state, which breaks the original time-translation symmetry because the subsequent time evolution takes place with the period $2\frac{2\pi}{\omega}$ [37]. The lifetime of the symmetry broken state goes to infinity when $N \to \infty$ but $\gamma =$ constant.

In the first part of this article, we do not consider spontaneous breaking of time-translation symmetry but we assume that the perfectly isolated system is prepared in the Floquet eigenstate $|\psi_+(t)\rangle = K(t,0)|\psi_+(0)\rangle$, where $K(t,0)$ is the time evolution operator corresponding to $\gamma < -1$, and $|\psi_+(0)\rangle$ is the Floquet eigenstate at $t = 0$. Subsequently, we assume that at $t = t_0 > 0$ the s-wave scattering length g_0 is suddenly changed to, e.g., zero. After the quench, the state evolves according to the new time evolution operator: $|\tilde{\psi}_+(t)\rangle = \tilde{K}(t,t_0)|\psi_+(t_0)\rangle$. Time evolution of $|\tilde{\psi}_+(t)\rangle$ can be easily obtained by numerical integration of the many-body Schrödinger equation with the Hamiltonian Eq. (1) (this Hamiltonian can be rewritten in the form of the spin system Hamiltonian [73] or the infinite-range Ising model [12]). However, it is much more instructive to apply the so-called continuum approximation [71], which reduces the many-body Hamiltonian Eq. (1) to the Hamiltonian of a fictitious particle,

$$\hat{H} = -\frac{J}{N}\sqrt{1-z^2}\frac{\partial^2}{\partial z^2} + V(z), \quad (2)$$

in the presence of the effective potential,

$$V(z) = \frac{JN}{2}\left(-\sqrt{1-z^2} + \frac{\gamma}{2}z^2\right). \quad (3)$$

Wave function $\psi(z)$ of the fictitious particle is a many-body state written in the Fock space basis $|N-n,n\rangle$ but with the assumption that number of particles N is so large that the relative population difference $z_n = \frac{(N-n)-n}{N}$ can be treated as a continuous variable z with the restriction $|z| \leqslant 1$.

There are two crucial ranges of the parameter γ. For $\gamma < -1$, the effective potential Eq. (3) possesses a double well structure, while for $\gamma > -1$ it has a single well shape [71]. For $\gamma < -1$, the ground state of the fictitious particle can be approximated by the superposition $\psi_+(z) = [\psi_L(z) + \psi_R(z)]/\sqrt{2}$, where $\psi_{L,R}$ are Gaussian states. (See Appendix A for a derivation of the continuum approximation, and the analytical solutions for $|\tilde{\psi}_+(t)\rangle$.) The state $\psi_+(z)$ is the previously described N-body Floquet eigenstate $|\psi_+(t)\rangle = \sum_n \psi_+(z_n)|N-n,n\rangle$ written in the time-dependent Fock basis and within the continuum approximation.

Let us assume that the system is prepared in the ground state $\psi(z) = \psi_+(z)$ of the Hamiltonian Eq. (2) for $\gamma < -1$ and at $t = t_0$ we suddenly set the scattering length g_0 to zero, i.e., we switch to $\gamma = 0$. The state $\tilde{\psi}(z, t > t_0)$ evolves according to the new Hamiltonian and we are interested in the so-called Loschmidt echo [14], i.e., the return probability to the initial state, $|\mathcal{G}(t > t_0)|^2$, where $\mathcal{G}(t) = \int_{-1}^{1} dz\psi_+^*(z)\tilde{\psi}(z,t)$. Such a Loschmidt echo corresponds actually to the return probability of the evolving N-body state $|\tilde{\psi}_+(t)\rangle = \sum_n \tilde{\psi}(z_n, t > t_0)|N-n,n\rangle$ to the time-periodic Floquet eigenstate $|\psi_+(t)\rangle$, i.e., $\mathcal{G}(t > t_0) = \langle\psi_+(t)|\tilde{\psi}_+(t)\rangle$. The Floquet eigenstate $|\psi_+(t)\rangle$ evolves periodically in time with the period $\frac{2\pi}{\omega}$ (modulo time-dependent global phase). The state $|\tilde{\psi}_+(t)\rangle$ also reveals nearly periodic behavior on short time intervals around any t; however, it becomes very quickly nearly orthogonal to $|\psi_+(t)\rangle$ if N is large. Dynamical quantum phase transitions are associated with nonanalytic behavior of the Loschmidt echo $|\mathcal{G}(t > t_0)|^2$. To study the quantum phase transitions in time, it is convenient to define an intensive rate function

$$\lambda_+(t) = \lim_{N\to\infty} \lambda_+^{(N)}(t), \quad \lambda_+^{(N)} = -N^{-1}\ln|\mathcal{G}(t)|^2. \quad (4)$$

In Fig. 1(a), we show the rate function $\lambda_+^{(N)}(t)$ obtained analytically within the continuum approximation, i.e., starting

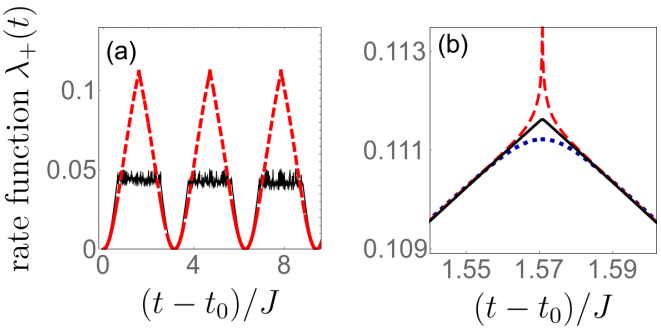

FIG. 1. Quench from $\gamma = -1.15$ to $\gamma = 0$ in the system prepared initially in the Floquet state $|\psi_+(t)\rangle$. Panel (a): The rate function $\lambda_+^{(N)}(t)$ obtained numerically (solid black line) and analytically within the continuum approximation (red dashed line) for $N = 1500$. Both curves follow each other except time intervals when the Loschmidt echo is so small that the numerical precision breaks down. Panel (b): Rate function $\lambda_+^{(N)}(t)$ for $N = 2\,000$ (blue dotted), 4 869 (red dashed), and 50 000 (black solid) in the vicinity of the critical time $t_c = t_0 + \frac{\pi}{2J}$. The diverging curve is related to an accidental value of N when the Loschmidt echo vanishes, cf. Eq. (6).

with $\psi(z,t_0) = [\psi_L(z) + \psi_R(z)]/\sqrt{2}$ for $\gamma = -1.15$ and $N = 1500$, we obtain subsequent evolution of $\tilde{\psi}(z,t > t_0)$ for $\gamma = 0$ by harmonic approximation of the potential Eq. (3) and by dropping $\sqrt{1-z^2}$ in Eq. (2). (See Appendix A for the derivation of the rate function $\lambda_+(t)$.) The analytical results follow closely the results of the full numerical integration of the N-body Schrödinger equation (also shown in Fig. 1) and allow us to obtain $\lambda_+^{(N)}(t)$ in regimes where the Loschmidt echo is so small that the numerical precision breaks down. Cusplike nonanalytic behavior of $\lambda_+(t)$ appear at critical times $t_c = t_0 + \frac{\pi}{2J}$ (modulo $\frac{\pi}{J}$). That is, one can show that $\frac{d}{dt}\lambda_+(t)$ is discontinuous,

$$\lim_{t\to t_c^{\pm}} \frac{d\lambda_+(t)}{dt} = \lim_{t\to t_c^{\pm}} \lim_{N\to\infty} \frac{d\lambda_+^{(N)}(t)}{dt} = \mp \frac{2q^2\Omega^3}{(1+\Omega^2)^2}, \tag{5}$$

where $\Omega = \sqrt{\gamma(1-\gamma^2)}(1-q^2)^{-1/4}$. It should be stressed that the order of the limits is important. Indeed, $\lim_{t\to t_c} \lambda_+(t)$ is well defined but

$$\lim_{N\to\infty} \lambda_+^{(N)}(t_c) = \frac{q^2\Omega}{1+\Omega^2} - \lim_{N\to\infty} \frac{1}{N} \ln\left[\cos^2\left(\frac{Nq^2\Omega^2}{2(1+\Omega^2)}\right)\right] \tag{6}$$

is not because whenever the cosine in Eq. (6) is close to zero, the logarithm diverges, which corresponds to accidental values of N for which the Loschmidt echo vanishes. In Fig. 1(b), we show $\lambda_+^{(N)}(t)$ around the first critical moment of time for different N. With the increasing particle number, we get closer to the nonanalytical behavior but, for some specific values of N, the rate diverges.

The Loschmidt echo can be interpreted as information about the evolving system from the point of view of the initial Floquet eigenstate. At the critical time, we are not able to extrapolate such information because of the breakdown of a short time expansion. Hilbert space of the system is spanned by the Fock states $|n_1,n_2\rangle$, where only two modes $\phi_{1,2}(x,t)$ are occupied by particles. It turns out that not only the Loschmidt echo but also

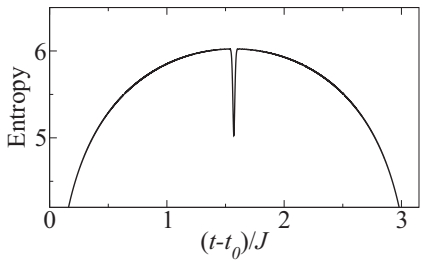

FIG. 2. Quench from $\gamma = -50$ to $\gamma = 0$ in the system of $N = 10^4$ particles prepared initially in the Floquet state $|\psi_+(t)\rangle$. Figure shows von Neumann entropy of the reduced density matrix of the system, i.e., $S(t > t_0) = -\mathrm{tr}(\rho_1 \ln \rho_1)$, where $\rho_1 = \sum_{n_2} \langle n_2|\tilde{\psi}_+(t)\rangle\langle\tilde{\psi}_+(t)|n_2\rangle$, after the quench. The results are obtained by numerical integration of the N-body Schrödinger equation. The jump of the entropy visible around the critical moment of time is consistent with Eq. (7).

the von Neumann entropy of the reduced density matrix of the system after the quench, i.e., $S(t > t_0) = -\mathrm{tr}(\rho_1 \ln \rho_1)$, where $\rho_1 = \sum_{n_2} \langle n_2|\tilde{\psi}_+(t)\rangle\langle\tilde{\psi}_+(t)|n_2\rangle$, reveals nonanalytical behavior at critical moments of time. Indeed, within the continuum approximation $S(t) = -\sum_n |\tilde{\psi}(z_n,t)|^2 \ln|\tilde{\psi}(z_n,t)|^2$ and

$$\lim_{t\to t_c^{\pm}} [S(t) - S(t_c)] \approx 1. \tag{7}$$

Figure 2 illustrates such a sudden jump of the entropy in the system of $N = 10^4$ particles; see Appendix B.

So far, we have considered the system prepared initially in the Floquet state $|\psi_+(t)\rangle$ that corresponds to the ground state of the Hamiltonian Eq. (1)—within the continuum approximation $\psi_+(z) = [\psi_L(z) + \psi_R(z)]/\sqrt{2}$. The first excited eigenstate of Eq. (1) can be approximated by $\psi_-(z) = [\psi_L(z) - \psi_R(z)]/\sqrt{2}$ and its eigenenergy becomes degenerate with the ground state energy when $N \to \infty$. If $\gamma \ll -1$, the Floquet state $|\psi_+(t)\rangle$ is actually a Schrödinger catlike state and it could be very difficult to prepare it experimentally because any loss of atoms makes the Schrödinger cat collapse to one of the states $|\psi_{L,R}(t)\rangle$ [37]. Assume that for $\gamma \ll -1$, we have prepared the system in the state $|\psi(t)\rangle = |\psi_R(t)\rangle = [|\psi_+(t)\rangle - |\psi_-(t)\rangle]/\sqrt{2}$, which is a symmetry broken state because it evolves with the period twice longer than $\frac{2\pi}{\omega}$ [37]. At $t = t_0$, we switch the scattering length g_0 to zero. If the ground state level of the initial Hamiltonian is degenerate, the Loschmidt echo is generalized to the return probability of the state after the quench to the ground state manifold [14,26], i.e.,

$$\mathcal{P}(t > t_0) = |\mathcal{G}_L(t)|^2 + |\mathcal{G}_R(t)|^2, \tag{8}$$

where $\mathcal{G}_{L,R}(t) = \langle\psi_{L,R}(t)|\tilde{\psi}(t)\rangle$. The rate function of the return probability reads

$$\lambda(t) = -\lim_{N\to\infty} N^{-1} \ln[\mathcal{P}(t)] = \min[\lambda_L(t),\lambda_R(t)], \tag{9}$$

where $\lambda_{L,R}(t) = \lim_{N\to\infty} \lambda_{L,R}^{(N)}$, $\lambda_{L,R}^{(N)} = -N^{-1} \ln|\mathcal{G}_{L,R}(t)|^2$.

Let us stress that the rate Eq. (9) defined for the initial symmetry broken state is the same as Eq. (4). Therefore, the observed cusps in $\lambda_+(t)$ are a direct consequence of the presence of two symmetry broken states and the fact that the rates $\lambda_{L/R}(t)$ cross at the critical time; see Appendix A. Let us also stress that, although the cusps of Loschmidt echo are difficult to measure, the rates can be easily accessible

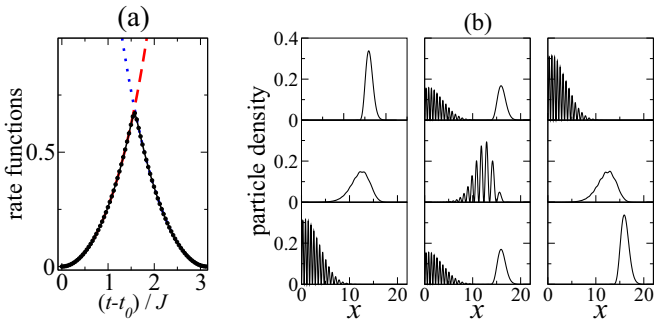

FIG. 3. Quench from $\gamma = -50$ to $\gamma = 0$ in the system of $N = 50$ particles bouncing on a mirror which is located at $x = 0$, where x is expressed in the gravitational units. The system is prepared initially in the symmetry broken state $|\psi(t)\rangle = |\psi_R(t)\rangle$. Panel (a): $\lambda_R^{(N)}$ (dashed red line) and $\lambda_L^{(N)}$ (dotted blue line) have been obtained by calculating the projections $|\langle\psi_{L,R}(t)|\tilde{\psi}(t)\rangle|^2$ while λ (black circles) has been determined from $-N^{-1}\ln[\mathcal{P}(t)]$. The results indicate that even for a relatively small particle number, $\lambda(t)$ coincides with $\min[\lambda_L^{(N)}(t),\lambda_R^{(N)}(t)]$. Panel (b): Left column illustrates evolution of the density of particles right after the quench, i.e., at t equal t_0, $t_0 + \frac{\pi}{\omega}$, and $t_0 + \frac{2\pi}{\omega}$ from top to bottom, respectively. Middle column presents the particle density at similar time moments, but around $t = t_c$, while the right column corresponds to analogues plots around $t = 2t_c$. One can see that in the middle column, both wave packets $\phi_{1,2}(x,t)$ are occupied by particles. At moments of time when the wave packets do not overlap, it is easy to determine their occupations by particles, $|\alpha_{1,2}|^2$, and, consequently, the rates $\lambda_{L,R}^{(N)} = -\ln|\alpha_{1,2}|^2$.

experimentally. Actually, in an experiment, it is not necessary to reach the thermodynamic limit in order to estimate nonanalyticities of the rate function $\lambda(t)$. Indeed, if $\lambda_{L,R}^{(N)}(t)$ measured the smallest value of them corresponds to $\lambda(t)$. This procedure has been adopted experimentally [27,28] and can be also applied in experiments on discrete time crystals. In Fig. 3(a), we show $\lambda_{L,R}^{(N)}(t)$ obtained in the case of a relatively small number of particles. The results confirm that $\lambda(t) \approx \min[\lambda_L^{(N)}(t),\lambda_R^{(N)}(t)]$. If initially we choose $\gamma \ll -1$, then at $t = t_0$ the system is a Bose-Einstein condensate where all bosons occupy the mode $\phi_2(x,t)$. At $t = t_c$ we have $\lambda_L(t) = \lambda_R(t)$, and consequently the return probabilities of $|\tilde{\psi}(t)\rangle$ to $|\psi_{L,R}(t)\rangle$ are equal. Nevertheless, this does not imply that a state $|\tilde{\psi}(t = t_c)\rangle$ is an equal superposition of $|\psi_{L,R}(t = t_c)\rangle$. In fact, we find that at all times the state is still a Bose-Einstein condensate with the wave function $\alpha_1\phi_1(x,t) + \alpha_2\phi_2(x,t)$. At $t = t_c$, the condensate wave function is an equal superposition of $\phi_1(x,t)$ and $\phi_2(x,t)$, and at $t = t_c + \frac{\pi}{2J}$, the mode $\phi_1(x,t)$ becomes a condensate wave function. Figure 3(b) illustrates evolution of atomic density: right after the quench, around the critical time $t_c = t_0 + \frac{\pi}{2J}$ and around $t = t_0 + \frac{\pi}{J}$. At moments of time when the wave packets $\phi_{1,2}(x,t)$ do not overlap, the measurement of atomic density allows one to obtain $\alpha_{1,2}$ and, consequently, the rates $\lambda_{L,R}^{(N)} = -\ln|\alpha_{1,2}|^2$.

III. CONCLUSIONS

In summary, we have shown that the dynamical quantum phase transitions are not restricted to time independent problems and can also occur in periodically driven systems. In particular, the dynamical quantum phase transitions can be observed in discrete time crystals. The Loschmidt echo is related to the return probability of the system after a quench to the initial periodically evolving Floquet eigenstate. We have shown that the first derivative of the rate function of the Loschmidt echo is discontinuous at $t = t_c$. The cusp in the Lochschmidt echo is a signature of passing the critical point between the discrete time crystal regime and the regime where no spontaneous time-translation symmetry breaking can be observed. Nonanalytical behavior of the corresponding rate function has been proven with the help of the so-called continuum approximation where the Hamiltonian of the many-body system is reduced to the one-body Hamiltonian of a fictitious particle. Dynamical quantum phase transition takes place in the thermodynamic limit, which corresponds to the infinite mass of the fictitious particle. The dynamical quantum phase transition described here can be observed in discrete time crystal experiments if the system is prepared in a state which reveals time-translation symmetry breaking.

ACKNOWLEDGMENT

Support of the National Science Centre, Poland via Projects No. 2016/21/B/ST2/01086 (A.K.) and No. 2016/21/B/ST2/01095 (K.S.) is acknowledged.

APPENDIX A: TIME EVOLUTION AFTER A QUENCH WITHIN THE CONTINUUM APPROXIMATION

In the main text, we consider a model of a discrete time crystal (DTC), whose description, in the periodically evolving basis, reduces to a N-body two-mode Hamiltonian

$$\hat{H} = -\frac{J}{2}(\hat{a}_1^\dagger\hat{a}_2 + \hat{a}_2^\dagger\hat{a}_1) + \frac{U}{2}(\hat{a}_1^\dagger\hat{a}_1^\dagger\hat{a}_1\hat{a}_1 + \hat{a}_2^\dagger\hat{a}_2^\dagger\hat{a}_2\hat{a}_2) + 2U_{12}\hat{a}_1^\dagger\hat{a}_1\hat{a}_2^\dagger\hat{a}_2, \tag{A1}$$

where $\hat{a}_{1,2}$ are standard bosonic operators which annihilate particles in the periodically evolving modes $\phi_{1,2}(x,t)$, J is hopping amplitude while U and U_{12} are interaction strengths between particles in the same and different modes, respectively. A relative interaction strength can be quantified by a dimensional parameter $\gamma = N(U - 2U_{12})/J$.

In the thermodynamical limit, i.e., where $N \to \infty$ but $\gamma =$ constant, the model has a quantum critial point at $\gamma = -1$, which separates a trivial and a DTC phase. In the DTC phase, i.e., for $\gamma < -1$, low-lying eigenstates of Eq. (A1) are vulnerable to any perturbation and spontaneous breaking of the discrete time translation can be observed [37,65].

Here, we describe the time evolution of the system when one starts with the DTC regime and prepares the system either in the symmetric ground state of Eq. (A1) or one of the lowest-symmetry broken states. After the quench through the quantum critical point to the trivial phase (i.e., to $\gamma = 0$) we observe singularities of the rate of the Loschmidt echo in time, see the main text. The after-quench evolution is described analytically within the so-called continuum approximation [71].

1. Continuous Hamiltonian

Let us write the Schrödinger equation of the system in the Fock basis

$$\langle n, N-n|\hat{H}|\psi\rangle = E\langle n, N-n|\psi\rangle, \tag{A2}$$

where $|\psi\rangle = \sum_n \psi_n |N-n,n\rangle$, or explicitly

$$\frac{JN}{2}\left[\psi_{n+1}\sqrt{\frac{1+z_n}{2}\left(\frac{1-z_n}{2}+\frac{1}{N}\right)} + \psi_{n-1}\sqrt{\frac{1-z_n}{2}\left(\frac{1+z_n}{2}+\frac{1}{N}\right)} - \frac{\gamma}{2}\psi_n z_n^2\right] = E\psi_n. \tag{A3}$$

For $N \gg 1$, we can treat the relative population difference $z_n = \frac{(N-n)-n}{N}$ as a continuous variable z with the condition that $|z| \leqslant 1$, and $\psi(z_n) = \psi_n$ as continuous wave function of a fictitious particle. The continuum approximation reduces the many-body Hamiltonian Eq. (A1) to

$$\hat{H} = -\frac{J}{N}\sqrt{1-z^2}\frac{\partial^2}{\partial z^2} + V(z), \tag{A4}$$

where the effective potential reads

$$V(z) = \frac{JN}{2}\left(-\sqrt{1-z^2} + \frac{\gamma}{2}z^2\right). \tag{A5}$$

For the latter convenience, we set $J = 1$.

2. Ground-state manifold

For $\gamma < -1$, the effective potential $V(z)$ has a double well structure and the lowest energy eigenstates of Eq. (A4) can be approximated by

$$\psi_\pm(z) = [\psi_L(z) \pm \psi_R(z)]/\sqrt{2}, \tag{A6}$$

where $\psi_{L,R}(z)$ are Gaussian states

$$\psi_{L,R}(z) = \frac{1}{(2\pi\sigma^2)^{1/4}} e^{-\frac{(z\pm q)^2}{4\sigma^2}}, \tag{A7}$$

where $q = \sqrt{1-\gamma^{-2}}, \sigma = 1/\sqrt{N\Omega}$ and $\Omega = \sqrt{\gamma(1-\gamma^2)}/(1-q^2)^{1/4}$. The Gaussian states are the harmonic oscillator ground states obtained by harmonic expansions of $V(z)$ around the two local minima $\pm q$

$$V(z \approx \pm q) \approx N\tilde{\Omega}^2(z \mp q)^2/4 + \text{const}, \tag{A8}$$

where $\tilde{\Omega} = \Omega(1-q^2)^{1/4}$ and by substituting $\sqrt{1-q^2}$ for $\sqrt{1-z^2}$ in Eq. (A4). For fixed γ, the larger N, the more localized Gaussian states because the total number of particles N is proportional to the mass of the fictitious particle described by the Hamiltonian Eq. (A4).

3. After-quench evolution

Let us assume that for large but finite N, the system is initially prepared in the symmetric ground state $\psi(z,0) = \psi_+(z)$ Eq. (A6). At $t = t_0 = 0$, we set $\gamma = 0$ and describe the time evolution of the system by means of the continuous Hamiltonian Eq. (A4), where the term $\sqrt{1-z^2}$ is neglected.

$$\tilde{\psi}(z,t) = \int dz' K(z,t;z')\psi_+(z), \tag{A9}$$

$$K(z,t;z') = \sqrt{\frac{a(t)}{\pi i}} e^{ia(t)[(z^2+z'^2)\cos(t)-2zz']}, \tag{A10}$$

where $a(t) = N/(4\sin(t))$. Explicitly, we obtain

$$\tilde{\psi}(z,t) = [\tilde{\psi}_L(z,t) + \tilde{\psi}_R(z,t)]/\sqrt{2}, \tag{A11}$$

$$\tilde{\psi}_{L,R}(z,t) = A(t)e^{-B(t)z^2 \pm iC(t)z + D(t)}, \tag{A12}$$

where

$$A(t) = \sqrt{\frac{-ia(t)}{b(t)\sqrt{2\pi\sigma^2}}}, \tag{A13}$$

$$B(t) = -a(t)\cos(t) + \frac{a(t)^2}{b(t)}, \tag{A14}$$

$$C(t) = \frac{|q|a(t)}{2\sigma^2 b(t)}, \tag{A15}$$

$$D(t) = \frac{q^2}{4\sigma^2}\left(-1 + \frac{1}{4\sigma^2 b(t)}\right), \tag{A16}$$

$$b(t) = \frac{1}{4\sigma^2} - ia(t)\cos(t). \tag{A17}$$

4. Loschmidt echo and rate function

In this part, we give explicit formulas, within the continuum approximation, for the Loschmidt echo and the rate function [29] when initially the system is prepared in the symmetric ground state Eq. (A6). The initial state is written in the periodically evolving basis and corresponds to the Floquet state that fulfils the discrete time-translation symmetry of the original time-dependent Hamiltonian.

The probability of the return of the evolving N-body state $|\tilde{\psi}_+(t)\rangle = \sum_n \tilde{\psi}(z_n, t > t_0)|N-n,n\rangle$ to the time-periodic Floquet symmetric eigenstate $|\psi_+(t)\rangle$ is given by the Loschmidt echo $|\mathcal{G}(t > t_0)|^2$, where

$$\mathcal{G}(t > t_0) = \langle\psi_+(t)|\tilde{\psi}_+(t)\rangle \tag{A18}$$

is called the Loschmidt amplitude. Within the continuum approximation, Eq. (A18) is equivalent to

$$\mathcal{G}(t) = \int \psi_+^*(z)\tilde{\psi}(z,t). \tag{A19}$$

The Loschmidt amplitude Eq. (A19) can be written in terms of the symmetry broken states Eqs. (A6) and (A11), namely

$$\begin{aligned}\mathcal{G}(t) &= \int \psi_L^*(z)\tilde{\psi}_L(z,t) + \int \psi_R^*(z)\tilde{\psi}_L(z,t)\\ &= \int \psi_R^*(z)\tilde{\psi}_R(z,t) + \int \psi_L^*(z)\tilde{\psi}_R(z,t)\\ &\equiv \mathcal{G}_R(t) + \mathcal{G}_L(t),\end{aligned} \tag{A20}$$

where, after a conscientious calculation we obtain

$$\mathcal{G}_R(t) = \sqrt{\frac{-ia(t)}{2\sigma^2 b(t)c(t)}} e^{-\frac{N}{2}(\lambda_R(t)+i\mu_R(t))}, \tag{A21}$$

$$\mathcal{G}_L(t) = \sqrt{\frac{-ia(t)}{2\sigma^2 b(t)c(t)}} e^{-\frac{N}{2}(\lambda_L(t)+i\mu_L(t))}, \tag{A22}$$

where

$$c(t) = -ia(t)\cos(t) + \frac{a(t)^2}{b(t)} + \frac{1}{4\sigma^2}, \tag{A23}$$

and

$$\lambda_R(t) = \frac{q^2\tilde{\Omega}\tan^2\left(\frac{t}{2}\right)}{\tilde{\Omega}^2 + \tan^2\left(\frac{t}{2}\right)}, \tag{A24}$$

$$\mu_R(t) = \frac{q^2\tilde{\Omega}^2\tan\left(\frac{t}{2}\right)}{\tilde{\Omega}^2 + \tan^2\left(\frac{t}{2}\right)}, \tag{A25}$$

$$\lambda_L(t) = \frac{q^2\tilde{\Omega}\cot^2\left(\frac{t}{2}\right)}{\tilde{\Omega}^2 + \cot^2\left(\frac{t}{2}\right)}, \tag{A26}$$

$$\mu_L(t) = \frac{-q^2\tilde{\Omega}^2\cot\left(\frac{t}{2}\right)}{\tilde{\Omega}^2 + \cot^2\left(\frac{t}{2}\right)}. \tag{A27}$$

The Loschmidt echo for noncritical states scales exponentially with the total number of particles N [74]. Therefore, it is convenient to consider an intensive quantity, i.e., the rate of the Loschmidt echo

$$\lambda_+(t) = \lim_{N\to\infty} \lambda_+^{(N)}(t), \quad \lambda_+^{(N)} = -N^{-1}\ln|\mathcal{G}(t)|^2. \tag{A28}$$

A straightforward calculation shows that in the thermodynamical limit,

$$\lambda_+(t) = \min\left(\lambda_R(t), \lambda_L(t)\right). \tag{A29}$$

The rate function Eq. (A29) has a nonanalytic cusp for $t = t_c = \pi/2$ when $\lambda_R = \lambda_L$. This cusp results in discontinuity of the first derivate of the rate function

$$\lim_{t\to t_c^{\pm}} \frac{d\lambda_+(t)}{dt} = \lim_{t\to t_c^{\pm}} \lim_{N\to\infty} \frac{d\lambda_+^{(N)}(t)}{dt} = \mp\frac{2q^2\Omega^3}{(1+\Omega^2)^2}. \tag{A30}$$

It should be stressed that the order of the limits is important. Indeed, $\lim_{t\to t_c} \lambda_+(t)$ is defined but

$$\lim_{N\to\infty} \lambda_+^{(N)}(t_c) = \frac{q^2\Omega}{1+\Omega^2} - \lim_{N\to\infty}\frac{1}{N}\ln\left[\cos^2\left(\frac{Nq^2\Omega^2}{2(1+\Omega^2)}\right)\right] \tag{A31}$$

is not because whenever the cosine in Eq. (A31) is close to zero, the logarithm diverges, which corresponds to accidental values of N for which the Loschmidt echo vanishes.

APPENDIX B: CALCULATION OF ENTANGLEMENT ENTROPY

In this section, we present the calculation of the nonanalytical jump of the entanglement entropy $S(t)$ at the critical point $t = t_c$ when the system is initially prepared in the symmetric Floquet state $\psi_+(z)$ Eq. (A6).

The von Neumann entropy of the reduced density matrix of the system after the quench is defined as

$$S(t > t_0) = -\mathrm{tr}(\rho_1 \ln \rho_1), \tag{B1}$$

where

$$\rho_1 = \sum_{n_2} \langle n_2|\tilde{\psi}_+(t)\rangle\langle\tilde{\psi}_+(t)|n_2\rangle. \tag{B2}$$

After decomposing the Floquet state in the Fock basis $|\tilde{\psi}_+(t)\rangle = \sum_n \tilde{\psi}(z_n,t)|n, N-n\rangle$, a straightforward calculation leads to

$$S(t) = -\sum_n |\tilde{\psi}(z_n,t)|^2 \ln|\tilde{\psi}(z_n,t)|^2. \tag{B3}$$

Let us first consider $S(t)$ away from the critical time. Applying the continuum approximation, we obtain

$$S(t\neq t_c) = -\int |\tilde{\psi}|^2\ln|\tilde{\psi}|^2 \approx \ln 2 + -\frac{1}{2}\left(\int |\tilde{\psi}_L|^2\ln|\tilde{\psi}_L|^2 + \int |\tilde{\psi}_R|^2\ln|\tilde{\psi}_R|^2\right), \tag{B4}$$

where we have used the fact that, away from the critical time, $|\tilde{\psi}|^2 \approx [|\tilde{\psi}_L|^2 + |\tilde{\psi}_R|^2]/2$ for $N \gg 1$. For sufficiently large N, Eq. (B4) holds for any t arbitrary close to t_c. In particular,

$$\lim_{t\to t_c^{\pm}} S(t\neq t_c) \approx \ln 2 - \int |\tilde{\psi}_0|^2\ln|\tilde{\psi}_0|^2, \tag{B5}$$

where, from Eqs. (A11)–(A12), we have

$$|\tilde{\psi}_0|^2 = \lim_{t\to t_c} |\tilde{\psi}_{L/R}|^2 = \sqrt{\frac{2}{\pi N\Omega}}\, e^{-Nz^2/(2\Omega)}. \tag{B6}$$

On the other hand, exactly at $t = t_c$ one gets

$$S(t_c) = -\int \left|\frac{\tilde{\psi}_0 e^{i\beta z} + \tilde{\psi}_0 e^{-i\beta z}}{\sqrt{2}}\right|^2 \ln\left|\frac{\tilde{\psi}_0 e^{i\beta z} + \tilde{\psi}_0 e^{-i\beta z}}{\sqrt{2}}\right|^2 \approx -\int |\tilde{\psi}_0|^2\ln|\tilde{\psi}_0|^2 - \int |\tilde{\psi}_0|^2\cos(2\beta z) + -2\int |\tilde{\psi}_0|^2\cos^2(\beta z)\ln[1+\cos(2\beta z)], \tag{B7}$$

where $\beta = Nq/2$. Note that because of the presence of $\cos^2(\beta z)$, there are no singular points under the integral in the second term. Subtracting Eq. (B7) from Eq. (B4) we obtain

$$\delta S(t_c) \equiv \lim_{t\to t_c^{\pm}} S(t\neq t_c) - S(t_c) \approx \ln 2 + 2\int |\tilde{\psi}_0|^2\cos(2\beta z) + \sum_{n=2}^{\infty}\int |\tilde{\psi}_0|^2 \frac{(-1)^n}{n(n-1)}\cos^n(2\beta z), \tag{B8}$$

where a series expansion of the logarithm was used. Highly oscillatory terms in Eq. (B8) can be dropped if $N \gg 1$. Note that

$$\cos^n(2\beta z) = \left(\frac{e^{2i\beta z} + e^{-2i\beta z}}{2}\right)^n = \sum_{k=0}^{n}\binom{n}{k}\frac{e^{2i\beta z(n-2k)}}{2^n}, \tag{B9}$$

and that the only nonoscillatory term in the sum Eq. (B9) corresponds to $k = n/2$. Using this result in Eq. (B8) we finally get

$$\delta S(t_c) \approx \ln 2 + \sum_{m=1}^{\infty}\binom{2m}{m}\frac{1}{2m(2m-1)4^m} = 1. \tag{B10}$$

[1] S. Sachdev, *Quantum Phase Transitions* (Cambridge University Press, Cambridge, 2011).
[2] S. Sachdev and B. Keimer, Phys. Today **64**, 29 (2011).
[3] M. Eckstein, M. Kollar, and P. Werner, Phys. Rev. Lett. **103**, 056403 (2009).
[4] J. P. Garrahan and I. Lesanovsky, Phys. Rev. Lett. **104**, 160601 (2010).
[5] S. Diehl, A. Tomadin, A. Micheli, R. Fazio, and P. Zoller, Phys. Rev. Lett. **105**, 015702 (2010).
[6] M. Schiró and M. Fabrizio, Phys. Rev. Lett. **105**, 076401 (2010).
[7] B. Sciolla and G. Biroli, Phys. Rev. Lett. **105**, 220401 (2010).
[8] B. Sciolla and G. Biroli, J. Stat. Mech.: Theory Exp. (2011) P11003.
[9] C. Ates, B. Olmos, J. P. Garrahan, and I. Lesanovsky, Phys. Rev. A **85**, 043620 (2012).
[10] B. Sciolla and G. Biroli, Phys. Rev. B **88**, 201110 (2013).
[11] R. Vosk and E. Altman, Phys. Rev. Lett. **112**, 217204 (2014).
[12] B. Žunkovič, A. Silva, and M. Fabrizio, Phil. Trans. R. Soc. A **374**, 20150160 (2016).
[13] A. Maraga, P. Smacchia, and A. Silva, Phys. Rev. B **94**, 245122 (2016).
[14] M. Heyl, A. Polkovnikov, and S. Kehrein, Phys. Rev. Lett. **110**, 135704 (2013).
[15] M. Heyl, Phys. Rev. Lett. **115**, 140602 (2015).
[16] J. C. Budich and M. Heyl, Phys. Rev. B **93**, 085416 (2016).
[17] S. Sharma, U. Divakaran, A. Polkovnikov, and A. Dutta, Phys. Rev. B **93**, 144306 (2016).
[18] U. Bhattacharya and A. Dutta, Phys. Rev. B **96**, 014302 (2017).
[19] U. Bhattacharya, S. Bandyopadhyay, and A. Dutta, Phys. Rev. B **96**, 180303 (2017).
[20] C. Karrasch and D. Schuricht, Phys. Rev. B **95**, 075143 (2017).
[21] M. Heyl and J. C. Budich, Phys. Rev. B **96**, 180304 (2017).
[22] J. C. Halimeh and V. Zauner-Stauber, Phys. Rev. B **96**, 134427 (2017).
[23] V. Zauner-Stauber and J. C. Halimeh, Phys. Rev. E **96**, 062118 (2017).
[24] I. Homrighausen, N. O. Abeling, V. Zauner-Stauber, and J. C. Halimeh, Phys. Rev. B **96**, 104436 (2017).
[25] J. Lang, B. Frank, and J. C. Halimeh, Phys. Rev. B **97**, 174401 (2018).
[26] B. Žunkovič, M. Heyl, M. Knap, and A. Silva, Phys. Rev. Lett. **120**, 130601 (2018).
[27] N. Fläschner, D. Vogel, M. Tarnowski, B. S. Rem, D.-S. Lühmann, M. Heyl, J. C. Budich, L. Mathey, K. Sengstock, and C. Weitenberg, Nat. Phys. **14**, 265 (2018).
[28] P. Jurcevic, H. Shen, P. Hauke, C. Maier, T. Brydges, C. Hempel, B. P. Lanyon, M. Heyl, R. Blatt, and C. F. Roos, Phys. Rev. Lett. **119**, 080501 (2017).
[29] M. Heyl, Rep. Prog. Phys. **81**, 054001 (2018).
[30] F. Wilczek, Phys. Rev. Lett. **109**, 160401 (2012).
[31] P. Bruno, Phys. Rev. Lett. **111**, 070402 (2013).
[32] H. Watanabe and M. Oshikawa, Phys. Rev. Lett. **114**, 251603 (2015).
[33] A. Syrwid, J. Zakrzewski, and K. Sacha, Phys. Rev. Lett. **119**, 250602 (2017).
[34] F. Iemini, A. Russomanno, J. Keeling, M. Schirò, M. Dalmonte, and R. Fazio, arXiv:1708.05014.
[35] Y. Huang, T. Li, and Z.-q. Yin, Phys. Rev. A **97**, 012115 (2018).
[36] N. V. Prokof'ev and B. V. Svistunov, arXiv:1710.00721.
[37] K. Sacha, Phys. Rev. A **91**, 033617 (2015).
[38] V. Khemani, A. Lazarides, R. Moessner, and S. L. Sondhi, Phys. Rev. Lett. **116**, 250401 (2016).
[39] D. V. Else, B. Bauer, and C. Nayak, Phys. Rev. Lett. **117**, 090402 (2016).
[40] N. Y. Yao, A. C. Potter, I.-D. Potirniche, and A. Vishwanath, Phys. Rev. Lett. **118**, 030401 (2017).
[41] A. Lazarides and R. Moessner, Phys. Rev. B **95**, 195135 (2017).
[42] A. Russomanno, F. Iemini, M. Dalmonte, and R. Fazio, Phys. Rev. B **95**, 214307 (2017).
[43] T.-S. Zeng and D. N. Sheng, Phys. Rev. B **96**, 094202 (2017).
[44] K. Nakatsugawa, T. Fujii, and S. Tanda, Phys. Rev. B **96**, 094308 (2017).
[45] W. W. Ho, S. Choi, M. D. Lukin, and D. A. Abanin, Phys. Rev. Lett. **119**, 010602 (2017).
[46] B. Huang, Y.-H. Wu, and W. V. Liu, Phys. Rev. Lett. **120**, 110603 (2018).
[47] Z. Gong, R. Hamazaki, and M. Ueda, Phys. Rev. Lett. **120**, 040404 (2018).
[48] R. R. W. Wang, B. Xing, G. G. Carlo, and D. Poletti, Phys. Rev. E **97**, 020202(R) (2018).
[49] J. Zhang, P. W. Hess, A. Kyprianidis, P. Becker, A. Lee, J. Smith, G. Pagano, I.-D. Potirniche, A. C. Potter, A. Vishwanath *et al.*, Nature **543**, 217 (2017).
[50] S. Choi, J. Choi, R. Landig, G. Kucsko, H. Zhou, J. Isoya, F. Jelezko, S. Onoda, H. Sumiya, V. Khemani *et al.*, Nature **543**, 221 (2017).
[51] C. Nayak, Nature **543**, 185 (2017).
[52] K. Kim, M.-S. Heo, K.-H. Lee, K. Jang, H.-R. Noh, D. Kim, and W. Jhe, Phys. Rev. Lett. **96**, 150601 (2006).
[53] M.-S. Heo, Y. Kim, K. Kim, G. Moon, J. Lee, H.-R. Noh, M. I. Dykman, and W. Jhe, Phys. Rev. E **82**, 031134 (2010).
[54] L. Guo, M. Marthaler, and G. Schön, Phys. Rev. Lett. **111**, 205303 (2013).
[55] K. Sacha, Sci. Rep. **5**, 10787 (2015).
[56] K. Sacha and D. Delande, Phys. Rev. A **94**, 023633 (2016).
[57] L. Guo and M. Marthaler, New J. Phys. **18**, 023006 (2016).
[58] L. Guo, M. Liu, and M. Marthaler, Phys. Rev. A **93**, 053616 (2016).
[59] K. Giergiel and K. Sacha, Phys. Rev. A **95**, 063402 (2017).
[60] M. Mierzejewski, K. Giergiel, and K. Sacha, Phys. Rev. B **96**, 140201 (2017).
[61] D. Delande, L. Morales-Molina, and K. Sacha, Phys. Rev. Lett. **119**, 230404 (2017).
[62] F. Flicker, arXiv:1707.09371.
[63] P. Liang, M. Marthaler, and L. Guo, New J. Phys. **20**, 023043 (2018).
[64] K. Giergiel, A. Miroszewski, and K. Sacha, Phys. Rev. Lett. **120**, 140401 (2018).
[65] K. Sacha and J. Zakrzewski, Rep. Prog. Phys. **81**, 016401 (2018).
[66] A. Steane, P. Szriftgiser, P. Desbiolles, and J. Dalibard, Phys. Rev. Lett. **74**, 4972 (1995).
[67] D. C. Lau, A. I. Sidorov, G. I. Opat, R. J. McLean, W. J. Rowlands, and P. Hannaford, Eur. Phys. J. D **5**, 193 (1999).
[68] K. Bongs, S. Burger, G. Birkl, K. Sengstock, W. Ertmer, K. Rzążewski, A. Sanpera, and M. Lewenstein, Phys. Rev. Lett. **83**, 3577 (1999).

[69] A. Buchleitner, D. Delande, and J. Zakrzewski, Phys. Rep. **368**, 409 (2002).
[70] S. Raghavan, A. Smerzi, S. Fantoni, and S. R. Shenoy, Phys. Rev. A **59**, 620 (1999).
[71] P. Ziń, J. Chwedeńczuk, B. Oleś, K. Sacha, and M. Trippenbach, Europhys. Lett. **83**, 64007 (2008).
[72] B. Oleś, P. Ziń, J. Chwedeńczuk, K. Sacha, and M. Trippenbach, Laser Phys. **20**, 671 (2010).
[73] G. J. Milburn, J. Corney, E. M. Wright, and D. F. Walls, Phys. Rev. A **55**, 4318 (1997).
[74] M. Heyl, Phys. Rev. B **95**, 060504 (2017).